Sohn, J-W., Harris, L. E., Berglund, E. D., Liu, T., Vong, L., Lowell, B. B., ... Elmquist, J. K. (2013). Melanocortin 4 Receptors Reciprocally Regulate Sympathetic and Parasympathetic Preganglionic Neurons. Cell, 152(3), 612-619. DOI: 10.1016/j.cell.2012.12.022

Cell

Melanocortin 4 Receptors Reciprocally Regulate Sympathetic and Parasympathetic Preganglionic Neurons

Jong-Woo Sohn,[1] Louise E. Harris,[3] Eric D. Berglund,[1] Tiemin Liu,[1] Linh Vong,[4] Bradford B. Lowell,[4] Nina Balthasar,[3,5,*] Kevin W. Williams,[1,5,*] and Joel K. Elmquist[1,2,5]
[1]Department of Internal Medicine
[2]Department of Pharmacology
Division of Hypothalamic Research, University of Texas Southwestern Medical Center at Dallas, Dallas, TX 75390, USA
[3]School of Physiology and Pharmacology, University of Bristol, Bristol BS8 1TD, UK
[4]Division of Endocrinology, Department of Medicine, Beth Israel Deaconess Medical Center and Harvard Medical School, Boston, MA 02115, USA
[5]These authors contributed equally to this work and are co-senior authors
*Correspondence: nina.balthasar@bristol.ac.uk (N.B.), kevin.williams@utsouthwestern.edu (K.W.W.)
http://dx.doi.org/10.1016/j.cell.2012.12.022

SUMMARY

Melanocortin 4 receptors (MC4Rs) in the central nervous system are key regulators of energy and glucose homeostasis. Notably, obese patients with MC4R mutations are hyperinsulinemic and resistant to obesity-induced hypertension. Although these effects are probably dependent upon the activity of the autonomic nervous system, the cellular effects of MC4Rs on parasympathetic and sympathetic neurons remain undefined. Here, we show that MC4R agonists inhibit parasympathetic preganglionic neurons in the brainstem. In contrast, MC4R agonists activate sympathetic preganglionic neurons in the spinal cord. Deletion of MC4Rs in cholinergic neurons resulted in elevated levels of insulin. Furthermore, re-expression of MC4Rs specifically in cholinergic neurons (including sympathetic preganglionic neurons) restores obesity-associated hypertension in MC4R null mice. These findings provide a cellular correlate of the autonomic side effects associated with MC4R agonists and demonstrate a role for MC4Rs expressed in cholinergic neurons in the regulation of insulin levels and in the development of obesity-induced hypertension.

INTRODUCTION

Obesity is correlated with an increased incidence of diabetes and hypertension while weight loss is often associated with decreases in blood glucose and blood pressure. A potential mediator of these processes is the central melanocortin system, which regulates food intake, energy expenditure, body weight, and glucose homeostasis via distinct projection patterns to melanocortin receptors in hypothalamic and extrahypothalamic nuclei (Cone, 2005). Importantly, mutations in melanocortin 4 receptors (MC4Rs) predispose both rodents and humans to obesity and diabetes independent of hypertension (Fan et al., 1997; Huszar et al., 1997; Tallam et al., 2005; Vaisse et al., 1998; Yeo et al., 1998). Moreover, MC4R agonists elevate blood pressure by increasing sympathetic activity (Greenfield et al., 2009; Kuo et al., 2004; Ni et al., 2006). Collectively, these findings predict that MC4Rs directly regulate autonomic neurons and potentially contribute to obesity-induced hypertension. Moreover, understanding the neurobiological mechanisms underlying MC4R activation in a distributed network of neurons (including the autonomic nervous system) may facilitate the advancement of novel treatments to prevent and/or treat obesity and its comorbidities.

Recent work demonstrated that re-expression of MC4Rs in the forebrain, including the paraventricular nucleus of the hypothalamus (PVH), and in the amygdala normalized the hyperphagia observed in MC4R null mice (Balthasar et al., 2005). This result was independent of effects on energy expenditure and glucose homeostasis (Balthasar et al., 2005). On the other hand, re-expression of MC4Rs in autonomic neurons normalized energy expenditure and glucose homeostasis (Rossi et al., 2011). Notably, MC4Rs restricted to the dorsal motor nucleus of vagus (DMV) have been suggested to regulate insulin secretion, while MC4Rs in the intermediolateral column (IML) modulate energy expenditure (Rossi et al., 2011). MC4R agonists lead to acute activation of neurons within the PVH and the dorsomedial nucleus of the hypothalamus (DMH) (Liu et al., 2003). Thus, direct activation of autonomic neurons expressing MC4Rs may lead to alterations in energy balance and glucose homeostasis. However, the physiological effects of activating both arms of the autonomic nervous system at the same time are not readily apparent. To address this issue, we assessed the cellular effects of MC4R agonists on parasympathetic and sympathetic neurons.

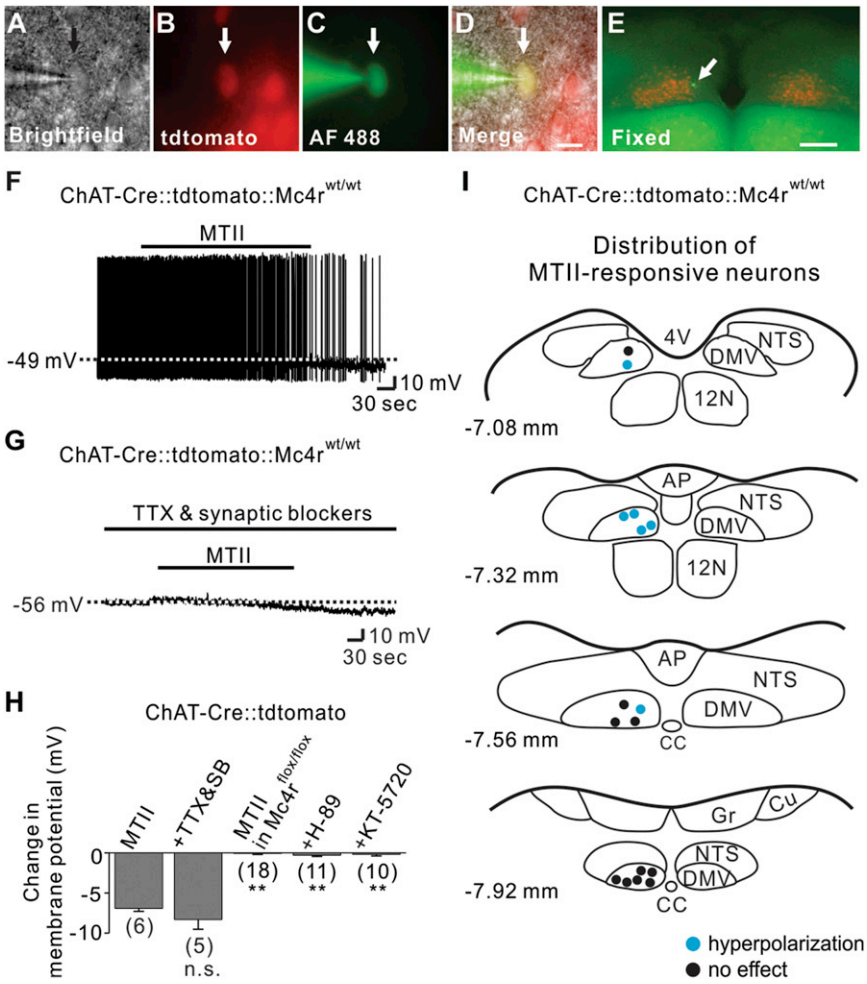

Figure 1. Parasympathetic Preganglionic Neurons of DMV Are Directly Inhibited by MC4Rs

(A–D) Brightfield illumination (A), fluorescent (TRITC) illumination (B), fluorescent (FITC) illumination (C), and merged image of targeted DMV cholinergic neuron (D, arrow indicates the targeted cell). Scale bar = 50 μm.

(E) Post hoc identification of recorded neuron within the DMV. Scale bar = 500 μm.

(F) Image demonstrates an MTII-induced hyperpolarization of DMV cholinergic neurons. Dashed line indicates the resting membrane potential.

(G) MTII hyperpolarized cholinergic neurons in the presence of TTX and fast synaptic blockers (CNQX, AP-5, picrotoxin).

(H) Histogram shows membrane potential changes of DMV cholinergic neurons. Numbers in parentheses indicate number of cells tested. Results are shown as means ± SEM. ** indicates $p < 0.01$.

(I) Images show the location of MTII-inhibited cholinergic neurons within the DMV (blue dots). 4V = fourth ventricle, AP = area postrema, CC = central canal, Cu = nucleus cuneatus, DMV = dorsal motor nucleus of vagus nerve, Gr = nucleus gracilis, and NTS = nucleus tractus solitarius. See also Figure S1.

RESULTS

MC4R Agonists Directly Inhibit Cholinergic Parasympathetic Preganglionic Neurons in the Brainstem

We used choline acetyltransferase (ChAT)-Cre::tdtomato reporter mice (Rossi et al., 2011) to examine the role of MC4Rs in acutely regulating the cellular activity of cholinergic neurons in the DMV. Acute coronal brainstem slices containing the DMV were prepared (Figures S1A and S1B) for electrophysiological recordings (Figures 1A–1D). In current clamp mode, MTII (an MC3R/4R agonist) hyperpolarized the membrane potential of cholinergic neurons within the DMV by −6.9 ± 0.4 mV (6/16, 37.5%; Figures 1F and 1H). The MTII-induced hyperpolarization was also observed in the presence of tetrodotoxin (TTX; 0.5 μM) and a cocktail of fast synaptic blockers (10 μM CNQX + 50 μM AP-5 + 50 μM picrotoxin), indicative of a postsynaptic mechanism (−8.3 ± 1.2 mV, n = 5, $t_{(9)}$ = 1.175; Figures 1G and 1H). Subsequent to the recordings, slices were fixed in order to identify the location of recorded cholinergic neurons within the rostrocaudal and mediolateral axis of DMV (Figure 1E). MTII-inhibited cholinergic neurons were located medially throughout the rostrocaudal axis of DMV (Figure 1I), and this pattern was conserved when pretreated by TTX/synaptic blockers (Figure S1C).

In order to further confirm the involvement MC4Rs, we generated mice in which cholinergic neurons were deficient in MC4Rs (ChAT-Cre::tdtomato::Mc4r$^{flox/flox}$, see Experimental Procedures). Biophysical properties of ChAT-Cre::tdtomato::Mc4r$^{flox/flox}$ cholinergic neurons were similar to wild-type cholinergic neurons (Figure 2A). Importantly, MTII failed to hyperpolarize the membrane potential of all DMV cholinergic neurons targeted from ChAT-Cre::tdtomato::Mc4r$^{flox/flox}$ mice (−0.1 ± 0.1 mV, n = 18, $t_{(22)}$ = 21.53; Figures 2B, 2C, and 1H). MC4Rs are coupled to Gs proteins (Mountjoy et al., 1994), which classically activate the adenylyl cyclase (AC)/cyclic AMP (cAMP)/protein kinase A (PKA) signaling pathways (Flagg et al., 2010). We confirmed that intracellular signaling pathways downstream of MC4Rs remained intact as pharmacological activation of AC/PKA by forskolin (10 μM) inhibited as well as activated cholinergic DMV neurons from ChAT-Cre::tdtomato::Mc4r$^{flox/flox}$ mice (Figures S2A and S2B). In a separate series of experiments, the MC4R-specific agonist, THIQ (100 nM), mimicked the hyperpolarizing effect of MTII (Figures S3A, S3D, and S3G). Similar to the effects of MTII, THIQ failed to influence the membrane potential of cholinergic neurons from ChAT-Cre::tdtomato::Mc4r$^{flox/flox}$ mice (Figures S3E–S3G). Together, these data support an MC4R-dependent hyperpolarization of cholinergic neurons within the DMV.

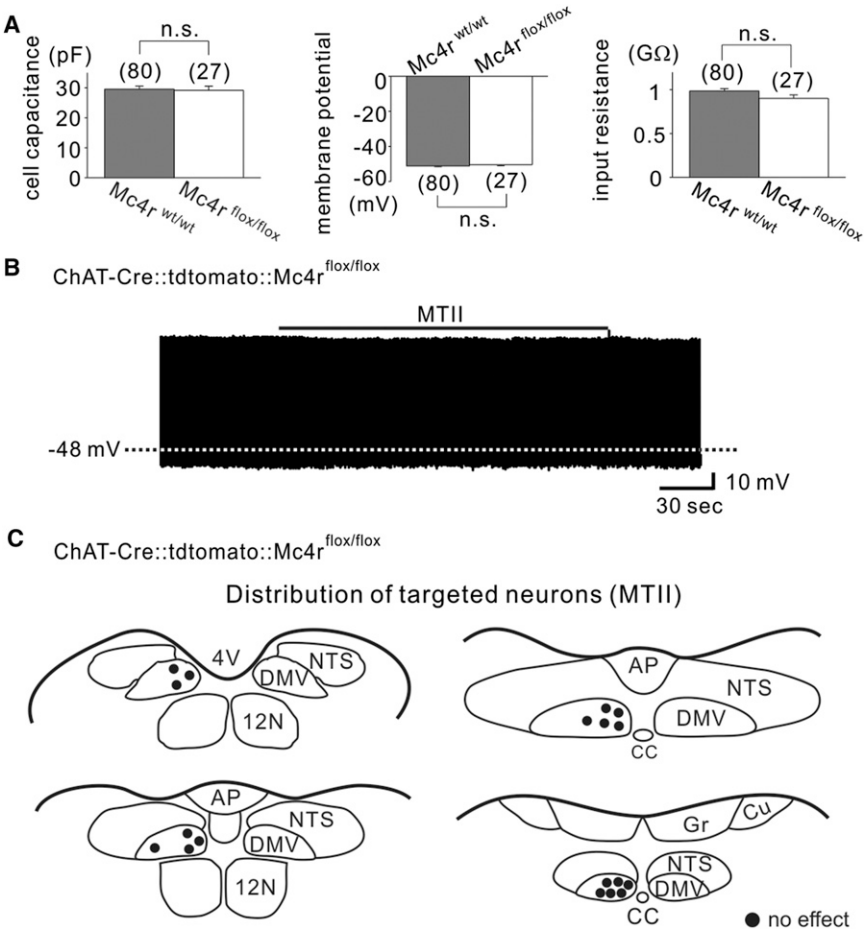

Figure 2. MC4R-Dependent Acute Inhibition of DMV Cholinergic Neurons

(A) Histograms demonstrating that cell capacitance, membrane potential, and input resistance were not significantly different between wild-type (gray) and MC4R-deficient (white) DMV cholinergic neurons. Results are shown as means ± SEM.

(B) MTII did not hyperpolarize cholinergic neurons in mice deficient for MC4Rs in ChAT-positive neurons.

(C) Drawings illustrate the location and the acute effect of MTII on targeted MC4R-deficient DMV cholinergic neurons.

See also Figures S2 and S3.

MC4R Agonists Inhibit DMV Cholinergic Neurons via a cAMP/PKA-Dependent Activation of a K_{ATP} Channel

The MTII-induced hyperpolarization of DMV cholinergic neurons was accompanied by a 16.8% ± 3.4% decrease in input resistance (n = 6, from 1,047 ± 75 MΩ to 871 ± 72 MΩ; E_{rev} = −106.1 ± 5.8 mV), suggesting the activation of a potassium channel (Figures 3B, 3C, and 3E). Moreover, the specific K_{ATP} channel inhibitor tolbutamide (200 μM) completely reversed the MTII-induced hyperpolarization in cholinergic DMV neurons (Figure 3A). Similar results were obtained with MTII in TTX/synaptic blockers (Figure 3E) and THIQ (Figures S3B, S3C, and S3H). Thus, MC4Rs inhibit cholinergic neurons in the DMV via activation of a putative K_{ATP} channel. Importantly, Gs protein-coupled receptors (GsPCRs) have been shown to cause vasodilation by activating K_{ATP} channels in vascular smooth muscle cells (Flagg et al., 2010; Quinn et al., 2004); however, this is the first demonstration of a similar mechanism within the CNS.

In order to examine the components of the signaling cascade in the GsPCR-coupled inhibition of DMV cholinergic neurons, we first examined whether direct activation of AC (using 10 μM forskolin) or PKA (using 500 μM 8-Br-cAMP) inhibited cholinergic neurons within the DMV. Similar to the effects of MTII and THIQ, superfusion of the AC activator (forskolin) hyperpolarized cholinergic neurons within the DMV (−8.1 ± 1.1 mV, 4 of 10; Figures S4A–S4C). Moreover, the PKA activator (8-Br-cAMP) hyperpolarized DMV cholinergic neurons (−8.2 ± 1.2 mV, 4 of 11; Figures S4D–S4F). The forskolin- and 8-Br-cAMP-induced hyperpolarization was completely reversed in the presence of tolbutamide, supporting the involvement of a putative K_{ATP} channel. Interestingly, in both experiments one cell was depolarized by either forskolin (Figures S4B and S4C) or 8-Br-cAMP (Figures S4E and S4F), suggesting that GsPCRs other than MC4Rs may activate cholinergic neurons within the DMV, as previously described (Wan et al., 2007). Pharmacological inhibition of PKA with either 1 μM H-89 or 100 nM KT-5720 completely blocked the MTII-induced hyperpolarization (Figures 1H, 3D, 3E, and S5). Together, these data suggest that MC4Rs activate postsynaptic PKA signaling pathways that open putative K_{ATP} channels ultimately leading to a direct hyperpolarization (inhibition) of parasympathetic preganglionic neurons in the DMV.

MC4R Agonists Suppress Excitatory Presynaptic Inputs to DMV Cholinergic Neurons

Recent evidence suggests that presynaptic terminals within the dorsal vagal complex (DVC) contain MC3R/4Rs (Wan et al., 2008). Thus, we tested the possibility that in addition to the direct postsynaptic effects of MC4Rs on DMV cholinergic neurons, MC4R agonists may also inhibit DMV cholinergic neurons via presynaptic mechanisms. We recorded miniature excitatory and inhibitory postsynaptic currents (mEPSCs and mIPSCs) using Cs^+-based pipette solutions (see Experimental Procedures). The mEPSC frequency was 2.3 ± 0.7 Hz (n = 14) throughout the rostrocaudal axis of DMV (Table 1). The MC4R-specific agonist, THIQ (100 nM), significantly decreased the frequency of mEPSCs in 9 of 14 cells recorded (from 3.0 ± 1.0 Hz in control ACSF to 2.1 ± 0.9 Hz in THIQ; 30% decrease, $t_{(8)}$ = 6.402 by paired t test, Table 1 and Figure S6A). The overall frequency of mEPSCs in the population was also significantly reduced in response to THIQ ($t_{(13)}$ = 5.214 by paired t test),

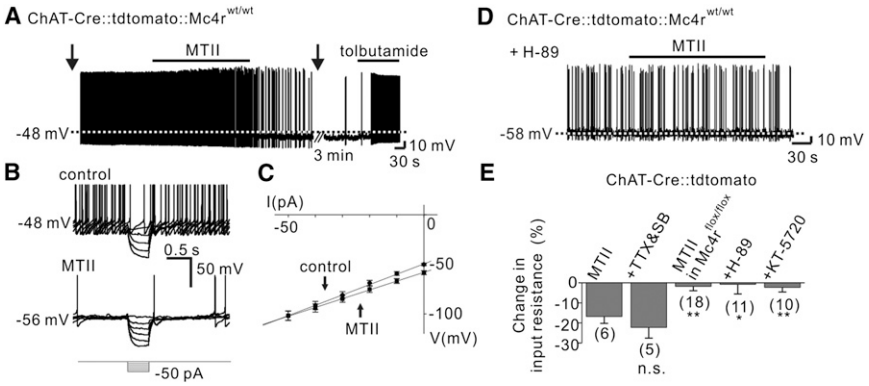

Figure 3. PKA-Dependent K_{ATP} Channel Activation Underlies the Acute Inhibition of DMV Neurons by MC4Rs

(A) Trace showing that MTII-induced hyperpolarization was completely reversed by tolbutamide. Arrows indicate interruption to apply current step pulses.

(B and C) MTII-induced decrease in input resistance as determined by small hyperpolarizing steps.

(D) MTII did not hyperpolarize cholinergic neurons when pretreated with H-89.

(E) Histogram shows input resistance changes of DMV cholinergic neurons. Numbers in parentheses indicate number of cells tested. Results are shown as means ± SEM. * indicates $p < 0.05$ and ** indicates $p < 0.01$.

See also Figures S4 and S5.

whereas the mean amplitude of mEPSCs was unaffected ($t_{(13)}$ = 0.1705 by paired t test). In contrast, THIQ either increased (three cells) or decreased (two cells) the frequency of mIPSCs (Figure S6B). The overall frequency and amplitude of mIPSCs in the population of recorded DMV cholinergic neurons were not significantly affected by THIQ ($t_{(12)}$ = 0.3474 and $t_{(12)}$ = 0.7079, respectively, by paired t test, Table 1). Interestingly, forskolin (10 μM) mimicked the effect of THIQ on mEPSCs frequency in three out of eight cells tested (45% decrease; Figure S6C). In the remaining neurons, mEPSC frequency was increased in one cell (65%) and was unchanged in the remaining four cells. These data support a model of an MC4R/cAMP-dependent decrease in excitatory tone to DMV cholinergic neurons, which contributes to a suppression of DMV cholinergic neuronal excitability.

MC4R Agonists Directly Activate Cholinergic Sympathetic Preganglionic Neurons in the Spinal Cord

We used ChAT-Cre::tdtomato reporter mice (Rossi et al., 2011) to examine the role of MC4Rs in acutely regulating the cellular activity of cholinergic neurons in the IML. Acute coronal spinal cord slices containing the IML (Figure S7A) were prepared for electrophysiological recordings (Figures 4A–4E). In contrast to the effects observed in DMV cholinergic neurons (Figures 1 and 3), but in agreement with results from neurons within the hypothalamus (Liu et al., 2003; Smith et al., 2007), the MC4R-specific agonist THIQ depolarized the membrane potential of IML cholinergic neurons (5 of 14; 5.4 ± 0.4 mV, Figures 4F and 4J). The depolarization by THIQ was accompanied by a 21.4% ± 2.0% decrease in input resistance (n = 5, from 962.4 ± 153.9 MΩ to 764.6 ± 128.1 MΩ; E_{rev} = −26.5 ± 2.4 mV), suggesting an activation of a putative nonselective cation conductance by THIQ (Figures 4H, 4I, and 4K). The THIQ-induced depolarization (4 of 10; 5.1 ± 0.2 mV, $t_{(7)}$ = 0.6504) and decrease in input resistance (22.9% ± 3.3%, n = 4, $t_{(7)}$ = 0.4114, from 1,329.8 ± 174.6 MΩ to 1,020.5 ± 133.1 MΩ; E_{rev} = −27.8 ± 3.5 mV) was also apparent in the presence of TTX and synaptic blockers, indicating a direct postsynaptic MC4R agonist-induced activation of IML cholinergic neurons (Figures 4G, 4J, and 4K). THIQ-activated cholinergic neurons were located medially within the IML, which was also conserved in slices pretreated with TTX and synaptic blockers (Figures S7B and S7C). These data demonstrate that MC4Rs activate a putative nonselective cationic channel that directly depolarizes (activates) sympathetic preganglionic neurons of IML.

Table 1. Effects of MC4R-Specific Agonist on Miniature Postsynaptic Currents Recorded from DMV Cholinergic Neurons

	Frequency (Hz)		Mean Amplitude (pA)	
	Control	THIQ	Control	THIQ
mEPSC (n=14)	2.3 ± 0.7	1.6 ± 0.6**	13.0 ± 0.9	12.8 ± 0.8
mIPSC (n=13)	1.2 ± 0.5	1.3 ± 0.6	14.2 ± 1.1	13.8 ± 1.1

See also Figure S6. ** indicates p<0.01 vs. control.

MC4Rs Specifically Expressed on Cholinergic Neurons Regulate Blood Pressure and Insulin Levels

Electrophysiological data suggest that MC4R signaling in cholinergic neurons decreases parasympathetic preganglionic neuronal activity in the brainstem while increasing sympathetic preganglionic neuronal activity in the spinal cord. To investigate the physiological effect of MC4R-mediated regulation of the autonomic nervous system in vivo, we measured mean arterial pressure in freely moving mice either lacking all MC4Rs (loxTB MC4R, Balthasar et al., 2005) or expressing MC4Rs only in Sim1-positive (Sim1-Cre, loxTB MC4R: PVH/amygdala, Balthasar et al., 2005) or ChAT-positive (ChAT-Cre, loxTB MC4R: cholinergic, Rossi et al., 2011) neurons, using radiotelemetry methods. Consistent with findings in MC4R knockout mice (Tallam et al., 2005) and obese human patients with MC4R mutations (Greenfield et al., 2009), we confirmed that mice lacking MC4Rs (loxTB MC4R mice) do not develop hypertension despite their obesity (black bars, Figures 5A and 5B). Interestingly, in contrast to Sim1-Cre, loxTB MC4R mice (light gray bars), ChAT-Cre, loxTB MC4R mice (dark gray bars) develop obesity-induced hypertension, which is only apparent during the animals' active nocturnal period (Figures 5A and 5B).

We previously demonstrated that reactivation of MC4Rs specifically in the cholinergic neurons normalizes hyperinsulinemia characteristic of MC4R deficiency (Rossi et al., 2011). In this study, we assessed the requirement of MC4Rs in the regulation of insulin levels. Selective deletion of MC4Rs in cholinergic

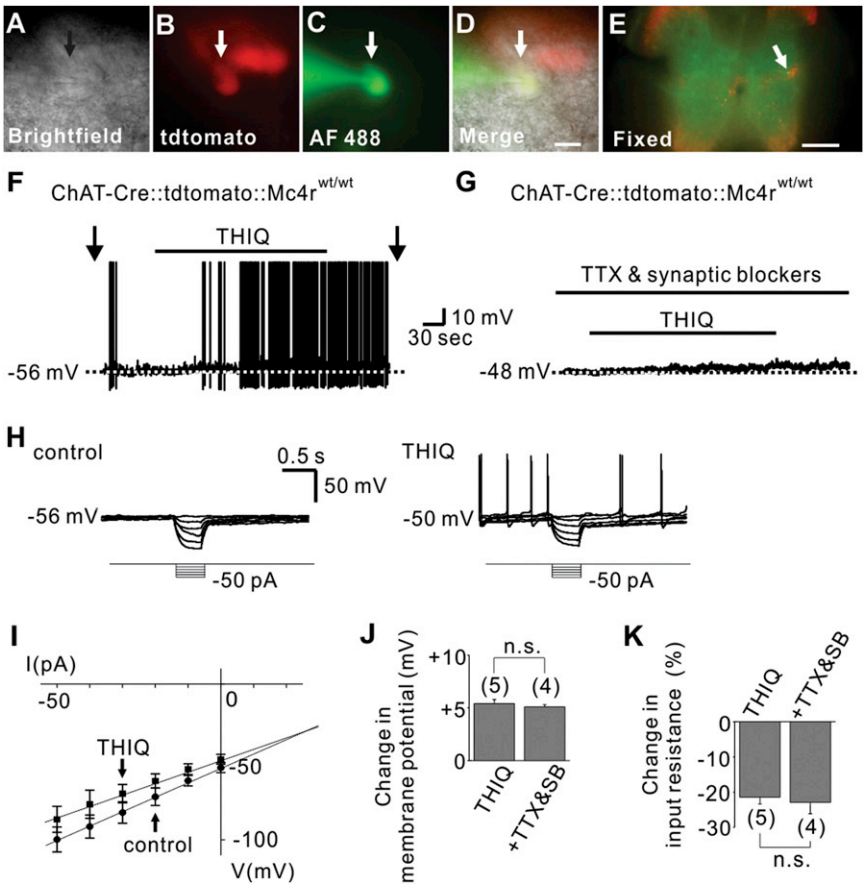

Figure 4. Sympathetic Preganglionic Neurons of IML Are Directly Activated by MC4Rs

(A–D) Brightfield illumination (A), fluorescent (TRITC) illumination (B), fluorescent (FITC) illumination (C), and merged image of targeted cholinergic IML neuron (D, arrow indicates the targeted cell). Scale bar = 50 μm.

(E) Post hoc identification of recorded neuron within IML. Scale bar = 500 μm.

(F) Trace shows a THIQ-induced depolarization of IML cholinergic neurons. Dashed line indicates the resting membrane potential.

(G) THIQ depolarized cholinergic neurons in the presence of TTX and fast synaptic blockers (CNQX, AP-5, picrotoxin).

(H and I) THIQ induced decrease in input resistance as determined by hyperpolarizing current steps.

(J and K) Histogram illustrates changes in membrane potential and input resistance of IML cholinergic neurons. Numbers in parentheses indicate number of cells tested. Results are shown as means ± SEM. See also Figure S7.

neurons (ChAT-Cre::Mc4r$^{flox/flox}$) resulted in significantly higher plasma insulin levels compared to weight-matched controls (Mc4r$^{flox/flox}$; $t_{(14)}$ = 7.396, Figure S2C). These results suggest that MC4Rs expressed by the cholinergic neurons are key regulators of blood insulin levels.

Discussion

In summary, these data demonstrate that MC4R agonists inhibit parasympathetic preganglionic neuronal activity while increasing sympathetic preganglionic neuronal activity through novel cellular mechanisms within the CNS (Figure 6). Notably, while Gs-coupled GPCRs in the CNS typically increase cellular and/or synaptic activity (Acuna-Goycolea and van den Pol, 2004; Diógenes et al., 2004; Lin et al., 2003; Liu et al., 2003; Pascoli et al., 2012; Smith et al., 2007; Wan et al., 2008; Wan et al., 2007), it is of particular interest that MC4Rs directly hyperpolarize DMV cholinergic neurons via cellular mechanisms identical to those found in vascular smooth muscle cells (Flagg et al., 2010; Quinn et al., 2004). Furthermore, we demonstrate that MC4R-mediated regulation of the autonomic nervous system plays a crucial role in the development of obesity-induced hypertension as well as the regulation of insulin levels.

Recent work demonstrated that mutations in MC4Rs resulted in obesity. However, the prevalence of hypertension was lower than in weight-matched obese patients without MC4R mutations, suggesting a protection against obesity-induced hypertension in MC4R mutant patients (Greenfield et al., 2009). Moreover, recent work suggests that stimulation of MC4Rs in obese patients is associated with hypertension (Greenfield et al., 2009). In support of these data, the present study suggests that stimulation of MC4Rs increases sympathetic tone which has been correlated with elevated blood pressure (Kuo et al., 2004; Ni et al., 2006). Indeed, re-expression of MC4Rs specifically in cholinergic neurons renders MC4R null mice hypertensive. Given our cellular data, it is likely that this is due to spinal cord MC4R-mediated increases in sympathetic tone. Re-expression of MC4Rs in Sim1-positive PVH/amygdala neurons had no effect on mean arterial pressure; note, however, that these mice are also not obese.

Obese children with MC4R mutations have elevated insulin levels (Farooqi et al., 2003). Interestingly, MC4Rs have also been suggested to regulate the release of insulin via the activity of sympathetic neurons (Fan et al., 2000; Obici et al., 2001). Moreover, recent evidence suggests an important role for MC4Rs in the DVC to regulate insulin secretion (Rossi et al., 2011). Consistent with this model, the present study suggests that activation of MC4Rs decreases parasympathetic tone, which may result in decreased insulin secretion. Importantly, we found that selective loss of MC4Rs in cholinergic neurons blunted the acute effects of MC4R agonists on cellular activity and also resulted in hyperinsulinemia.

Together, these data demonstrate a reciprocal regulation of sympathetic and parasympathetic activity by MC4Rs. These findings provide further evidence for the effects of MC4Rs in the autonomic nervous system to decrease insulin secretion while increasing energy expenditure and blood pressure. These

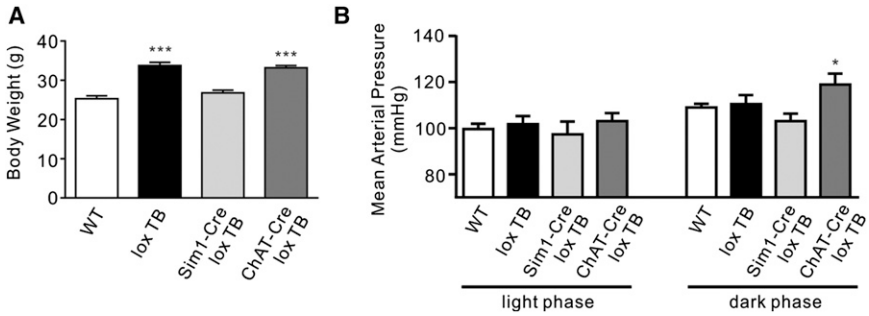

Figure 5. Re-expression of MC4Rs Specifically on Cholinergic Neurons Renders Mice Hypertensive

(A) Body weight data (means ± SEM). n = 5–9 per group, one-way ANOVA ***p < 0.001.

(B) Radiotelemetry recordings in ad libitum chow fed, freely moving 8–10 week-old wild-type, loxTB MC4R, Sim1-cre, loxTB MC4R, and ChAT-Cre, loxTB MC4R mice. Measurements were taken for 5 min every hour over a 72 hr period; presented are average (means ± SEM) light- and dark-phase values for mean arterial pressure. (n = 5–9 per group, *p < 0.05 two-way repeated-measures ANOVA).

data also provide a molecular and cellular mechanism for the role of MC4Rs in the regulation of the autonomic nervous system. Notably, these cellular/molecular observations are linked to physiological outcomes and demonstrate that MC4Rs on cholinergic neurons indeed play an important role in obesity-induced hypertension. Consequently, these observations may contribute to the development of novel therapeutic strategies in the treatment of obesity and associated comorbidities such as diabetes and hypertension.

EXPERIMENTAL PROCEDURES

Mice

Mice in which Cre expression was restricted to cholinergic neurons (ChAT-IRES-Cre or ChAT-Cre mice) (Rossi et al., 2011) were mated with tdtomato reporter mouse (Jackson Laboratory, #007908) in order to identify the autonomic preganglionic neurons. For some experiments, ChAT-Cre::tdtomato reporter mice or ChAT-Cre mice were subsequently mated with $Mc4r^{flox/flox}$ mice in order to generate mice selectively deficient in MC4Rs in cholinergic neurons. $Mc4r^{flox/flox}$ mice were made by inserting loxP sites to flank the single exon (5′loxP site into 5′UTR—similar to where the loxTB cassette sits in the loxTB MC4R mouse—the 3′loxP site sits after the 3′UTR). $Mc4r^{flox/flox}$ homozygous mice were bred to EIIA-Cre to produce MC4R null mice ($Mc4r^{\Delta/\Delta}$). $Mc4r^{\Delta/\Delta}$ mice were obese with increased linear length and lean mass, similar to what was reported for MC4R null mice (Huszar et al., 1997) and also for the loxTB MC4R mice (Balthasar et al., 2005). A full description of the $Mc4r^{flox/flox}$ mice will appear in a subsequent manuscript by L.V. and B.B.L.

All mice used for electrophysiological recordings were housed in a light-dark (12 hr on/off; lights on at 7:00 a.m.) and temperature-controlled environment with food and water available ad libitum in the University of Texas Southwestern Medical Center Facility. For radiotelemetry, the loxTB MC4R (Balthasar et al., 2005), Sim1-Cre, loxTB MC4R (Balthasar et al., 2005), and ChAT-Cre, loxTB MC4R (Rossi et al., 2011) mice and their wild-type littermates were maintained on a mouse chow (2016 Teklad Global 16% Protein Rodent Diet, Harlan, UK) at the University of Bristol Facility. All experiments were performed in accordance with the guidelines established by the National Institute of Health Guide for the Care and Use of Laboratory Animals, the University of Texas Southwestern Medical Center Institutional Animal Care and Use Committee, the UK Animals (Scientific Procedures) Act, and the University of Bristol Ethical Review Group.

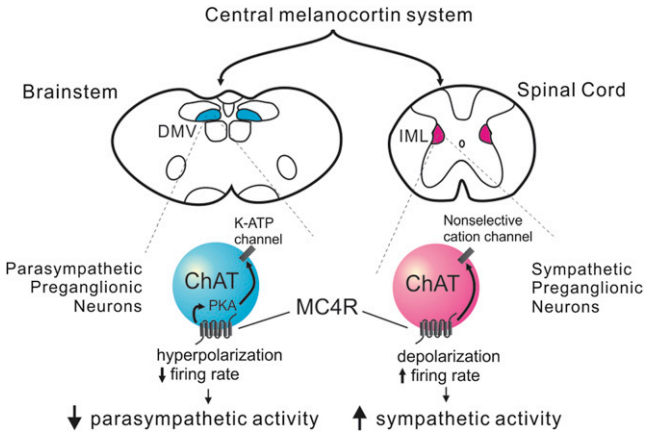

Figure 6. The Central Melanocortin System Decreases Parasympathetic Activity and Increases Sympathetic Activity via Direct Activation of MC4Rs

The central melanocortin system innervates parasympathetic preganglionic (DMV) and sympathetic preganglionic (IML) neurons, both of which express MC4Rs. DMV cholinergic neurons are inhibited by MC4Rs via a PKA-dependent activation of putative K_{ATP} channels, whereas IML cholinergic neurons are activated via an MC4R-induced activation of a putative nonselective cation channel. The altered cellular activity supports an MC4R-dependent suppression of parasympathetic activity and enhancement of sympathetic activity, which has implications for a variety of disease states including diabetes and hypertension.

Electrophysiology

Whole-cell patch-clamp recordings from cholinergic neurons maintained in brainstem or thoracic spinal cord slice preparations were performed as previously described (Hill et al., 2008; Wang et al., 2008; Williams and Smith, 2006; Williams et al., 2007). Briefly, 4- to 14-week-old male mice were deeply anesthetized with i.p. injection of 7% chloral hydrate and transcardially perfused with a modified ice-cold artificial cerebrospinal fluid (ACSF) (described below), in which an equiosmolar amount of sucrose was substituted for NaCl. The mice were then decapitated, and the entire brainstem or thoracic spinal cord was removed and immediately submerged in ice cold, carbogen-saturated (95% O_2 and 5% CO_2) ACSF (126 mM NaCl, 2.8 mM KCl, 1.2 mM $MgCl_2$, 2.5 mM $CaCl_2$, 1.25 mM NaH_2PO_4, 26 mM $NaHCO_3$, and 5 mM glucose). A brain block containing the brainstem or thoracic spinal cord glued to agarose blocks was mounted on a stage. Coronal sections (200–350 μm) were cut from either the medulla oblongata containing the DMV or the upper thoracic spinal cord containing the IML with a Leica VT1000S Vibratome and then incubated in oxygenated ACSF at room temperature for at least 1 hr before recording. Slices were transferred to the recording chamber and allowed to equilibrate for 10–20 min before recording. The slices were bathed in oxygenated ACSF (32°C–34°C) at a flow rate of ~2 ml/min.

The pipette solution for current-clamp whole-cell recording was modified to include an intracellular dye (Alexa Fluor 488): 120 mM K-gluconate, 10 mM KCl, 10 mM HEPES, 5 mM EGTA, 1 mM $CaCl_2$, 1 mM $MgCl_2$, 2 mM MgATP, and 0.03 mM Alexa Fluor 488 hydrazide dye (pH 7.3). K-gluconate was replaced by equimolar Cs-gluconate for voltage-clamp experiments recording mEPSCs and mIPSCs. Epifluorescence was briefly used to target fluorescent cells, at which time the light source was switched to infrared differential interference contrast imaging to obtain the whole-cell recording (Zeiss Axioskop FS2 Plus or Nikon Eclipse FN1 equipped with a fixed stage and a

QuantEM:512SC electron-multiplying charge-coupled device camera). Electrophysiological signals were recorded using an Axopatch 700B amplifier (Molecular Devices), low-pass filtered at 2–5 kHz, and analyzed offline on a PC with pCLAMP programs (Molecular Devices). Recording electrodes had resistances of 2.5–5 MΩ when filled with the K-gluconate or Cs-gluconate internal solutions. mEPSCs were recorded as inward currents at a holding potential of −60 mV, and mIPSCs were recorded as outward currents at a holding potential of −10 mV, as described previously (Williams and Smith, 2006; Williams et al., 2007). Input resistance was assessed by measuring voltage deflection at the end of the response to hyperpolarizing rectangular current pulse steps (500 ms of −10 to −50 pA). Membrane potential values were compensated to account for junction potential (−8 mV).

MTII (100 nM, Bachem) and THIQ (100 nM, Tocris) were added to the ACSF for specific experiments. Solutions containing MTII or THIQ were typically perfused for 3–5 min. A drug effect was required to be associated temporally with peptide application, and the response had to be stable within a few minutes. A neuron was considered depolarized or hyperpolarized if a change in membrane potential was at least 2 mV in amplitude. After recording, slices were fixed with 4% formalin in PBS at 4°C overnight. After washing in PBS, slices were mounted onto slides, covered in Vectashield (Vector Laboratories), and coverslipped to reduce photo-oxidation during visualization with fluorescent light. Cells were then visualized with ApoTome imaging system (Imager Z1; Zeiss) to identify post hoc the anatomical location of the recorded neuron within the DMV or the IML.

Drugs

TTX, H-89, KT-5702, forskolin, and 8-Br-cAMP were obtained from Tocris. CNQX, AP-5, and picrotoxin were obtained from Sigma. All solutions were made according to manufacturer specifications. Stock solutions of KT-5720 and forskolin were made by dissolution in DMSO (Sigma). The concentration of DMSO in the external solution was < 0.1%. Stock solutions of MTII were made by dissolution in PBS (GIBCO). Stock solutions of THIQ, TTX, CNQX, AP-5, picrotoxin, H-89, and 8-Br-cAMP were made by dissolution in deionized water.

Radiotelemetry

Mice were surgically fitted with a Data Sciences International (Minnesota, USA) TAIIPA-C10 small rodent radio transmitter in the left carotid artery. Ten days after recovery, single-caged mice were placed on receiver pads in their home cage with free access to food and water. Data were collected and analyzed using Dataquest A.R.T. 4.0 software (DSI, Minnesota, USA). Baseline cardiovascular measurements were taken for 5 min every hour over a 72 hr period, separated into light (7 a.m. – 5 p.m.) and dark (7 p.m. – 5 a.m.) phase, and averaged over the 72 hr.

Basal Insulin Levels

Basal insulin levels were measured in male mice at 3 months of age. Mice were transferred to a clean cage containing water but no food at 8 a.m. to begin a 5 hr fast. Blood samples were then collected from the cut tail and centrifuged, and plasma was removed as the supernatant. Plasma insulin levels were measured using an ELISA kit (Crystal Chem, Downers Grove, IL) according to manufacturer's instruction.

Data Analysis

Statistical data are expressed as means ± SEM, where n represents the number of cells studied. The significance of differences between measurements was evaluated using unpaired two-tailed Student's t test with a confidence level of $p < 0.05$ (*) or $p < 0.01$ (**). For Figures 5A and 5B significance was evaluated using one-way ANOVA or two-way repeated-measures ANOVA, respectively, with relevant post hoc tests. For the analysis of PSCs, at least 2 min recording of mEPSCs and mIPSCs was examined to identify drug effects on amplitude and frequency distributions. A value of twice the mean peak-to-peak noise level for a given recording in control solutions was used as the detection limit for minimal PSC amplitude (i.e., typically 5–10 pA). Drug effects on miniature PSC frequency before and during drug application were analyzed within a recording using the Kolmogorov-Smirnov (K-S) test (a nonparametric, distribution-free goodness-of-fit test for probability distributions). Pooled results of miniature PSC frequency and drug effects on mean amplitude of miniature PSCs were analyzed using a paired two-tailed t test with a confidence level of $p < 0.05$ (*) or $p < 0.01$ (**).

SUPPLEMENTAL INFORMATION

Supplemental Information includes seven figures and can be found with this article online at http://dx.doi.org/10.1016/j.cell.2012.12.022.

ACKNOWLEDGMENTS

This work was supported by the American Diabetes Association 07-11-MN-16 (J.K.E. and T.L.); American Heart Association 12POST8860007 (J.-W.S.); British Heart Foundation FS/06/057 (N.B.); Lister Institute for Preventive Medicine (N.B.); National Institutes of Health F32 DK092083 (E.D.B), K01 DK087780 (K.W.W.), P01 DK088761(J.K.E.), RL1 DK081185 (J.K.E.), R37 DK053301 (J.K.E.), F32 DK078478 (L.V.), and R01 DK075632 (B.B.L.), P30 DK046200 (B.B.L.), and P30 DK057521 (B.B.L.).

Received: September 4, 2012
Revised: November 20, 2012
Accepted: December 18, 2012
Published: January 31, 2013

REFERENCES

Acuna-Goycolea, C., and van den Pol, A. (2004). Glucagon-like peptide 1 excites hypocretin/orexin neurons by direct and indirect mechanisms: implications for viscera-mediated arousal. J. Neurosci. *24*, 8141–8152.

Balthasar, N., Dalgaard, L.T., Lee, C.E., Yu, J., Funahashi, H., Williams, T., Ferreira, M., Tang, V., McGovern, R.A., Kenny, C.D., et al. (2005). Divergence of melanocortin pathways in the control of food intake and energy expenditure. Cell *123*, 493–505.

Cone, R.D. (2005). Anatomy and regulation of the central melanocortin system. Nat. Neurosci. *8*, 571–578.

Diógenes, M.J., Fernandes, C.C., Sebastião, A.M., and Ribeiro, J.A. (2004). Activation of adenosine A2A receptor facilitates brain-derived neurotrophic factor modulation of synaptic transmission in hippocampal slices. J. Neurosci. *24*, 2905–2913.

Fan, W., Boston, B.A., Kesterson, R.A., Hruby, V.J., and Cone, R.D. (1997). Role of melanocortinergic neurons in feeding and the agouti obesity syndrome. Nature *385*, 165–168.

Fan, W., Dinulescu, D.M., Butler, A.A., Zhou, J., Marks, D.L., and Cone, R.D. (2000). The central melanocortin system can directly regulate serum insulin levels. Endocrinology *141*, 3072–3079.

Farooqi, I.S., Keogh, J.M., Yeo, G.S., Lank, E.J., Cheetham, T., and O'Rahilly, S. (2003). Clinical spectrum of obesity and mutations in the melanocortin 4 receptor gene. N. Engl. J. Med. *348*, 1085–1095.

Flagg, T.P., Enkvetchakul, D., Koster, J.C., and Nichols, C.G. (2010). Muscle KATP channels: recent insights to energy sensing and myoprotection. Physiol. Rev. *90*, 799–829.

Greenfield, J.R., Miller, J.W., Keogh, J.M., Henning, E., Satterwhite, J.H., Cameron, G.S., Astruc, B., Mayer, J.P., Brage, S., See, T.C., et al. (2009). Modulation of blood pressure by central melanocortinergic pathways. N. Engl. J. Med. *360*, 44–52.

Hill, J.W., Williams, K.W., Ye, C., Luo, J., Balthasar, N., Coppari, R., Cowley, M.A., Cantley, L.C., Lowell, B.B., and Elmquist, J.K. (2008). Acute effects of leptin require PI3K signaling in hypothalamic proopiomelanocortin neurons in mice. J. Clin. Invest. *118*, 1796–1805.

Huszar, D., Lynch, C.A., Fairchild-Huntress, V., Dunmore, J.H., Fang, Q., Berkemeier, L.R., Gu, W., Kesterson, R.A., Boston, B.A., Cone, R.D., et al. (1997). Targeted disruption of the melanocortin-4 receptor results in obesity in mice. Cell *88*, 131–141.

Kuo, J.J., da Silva, A.A., Tallam, L.S., and Hall, J.E. (2004). Role of adrenergic activity in pressor responses to chronic melanocortin receptor activation. Hypertension *43*, 370–375.

Lin, Y.W., Min, M.Y., Chiu, T.H., and Yang, H.W. (2003). Enhancement of associative long-term potentiation by activation of beta-adrenergic receptors at CA1 synapses in rat hippocampal slices. J. Neurosci. *23*, 4173–4181.

Liu, H., Kishi, T., Roseberry, A.G., Cai, X., Lee, C.E., Montez, J.M., Friedman, J.M., and Elmquist, J.K. (2003). Transgenic mice expressing green fluorescent protein under the control of the melanocortin-4 receptor promoter. J. Neurosci. *23*, 7143–7154.

Mountjoy, K.G., Mortrud, M.T., Low, M.J., Simerly, R.B., and Cone, R.D. (1994). Localization of the melanocortin-4 receptor (MC4-R) in neuroendocrine and autonomic control circuits in the brain. Mol. Endocrinol. *8*, 1298–1308.

Ni, X.P., Butler, A.A., Cone, R.D., and Humphreys, M.H. (2006). Central receptors mediating the cardiovascular actions of melanocyte stimulating hormones. J. Hypertens. *24*, 2239–2246.

Obici, S., Feng, Z., Tan, J., Liu, L., Karkanias, G., and Rossetti, L. (2001). Central melanocortin receptors regulate insulin action. J. Clin. Invest. *108*, 1079–1085.

Pascoli, V., Turiault, M., and Lüscher, C. (2012). Reversal of cocaine-evoked synaptic potentiation resets drug-induced adaptive behaviour. Nature *481*, 71–75.

Quinn, K.V., Giblin, J.P., and Tinker, A. (2004). Multisite phosphorylation mechanism for protein kinase A activation of the smooth muscle ATP-sensitive K+ channel. Circ. Res. *94*, 1359–1366.

Rossi, J., Balthasar, N., Olson, D., Scott, M., Berglund, E., Lee, C.E., Choi, M.J., Lauzon, D., Lowell, B.B., and Elmquist, J.K. (2011). Melanocortin-4 receptors expressed by cholinergic neurons regulate energy balance and glucose homeostasis. Cell Metab. *13*, 195–204.

Smith, M.A., Hisadome, K., Al-Qassab, H., Heffron, H., Withers, D.J., and Ashford, M.L. (2007). Melanocortins and agouti-related protein modulate the excitability of two arcuate nucleus neuron populations by alteration of resting potassium conductances. J. Physiol. *578*, 425–438.

Tallam, L.S., Stec, D.E., Willis, M.A., da Silva, A.A., and Hall, J.E. (2005). Melanocortin-4 receptor-deficient mice are not hypertensive or salt-sensitive despite obesity, hyperinsulinemia, and hyperleptinemia. Hypertension *46*, 326–332.

Vaisse, C., Clement, K., Guy-Grand, B., and Froguel, P. (1998). A frameshift mutation in human MC4R is associated with a dominant form of obesity. Nat. Genet. *20*, 113–114.

Wan, S., Coleman, F.H., and Travagli, R.A. (2007). Glucagon-like peptide-1 excites pancreas-projecting preganglionic vagal motoneurons. Am. J. Physiol. Gastrointest. Liver Physiol. *292*, G1474–G1482.

Wan, S., Browning, K.N., Coleman, F.H., Sutton, G., Zheng, H., Butler, A., Berthoud, H.R., and Travagli, R.A. (2008). Presynaptic melanocortin-4 receptors on vagal afferent fibers modulate the excitability of rat nucleus tractus solitarius neurons. J. Neurosci. *28*, 4957–4966.

Wang, L., Spary, E., Deuchars, J., and Deuchars, S.A. (2008). Tonic GABAergic inhibition of sympathetic preganglionic neurons: a novel substrate for sympathetic control. J. Neurosci. *28*, 12445–12452.

Williams, K.W., and Smith, B.N. (2006). Rapid inhibition of neural excitability in the nucleus tractus solitarii by leptin: implications for ingestive behaviour. J. Physiol. *573*, 395–412.

Williams, K.W., Zsombok, A., and Smith, B.N. (2007). Rapid inhibition of neurons in the dorsal motor nucleus of the vagus by leptin. Endocrinology *148*, 1868–1881.

Yeo, G.S., Farooqi, I.S., Aminian, S., Halsall, D.J., Stanhope, R.G., and O'Rahilly, S. (1998). A frameshift mutation in MC4R associated with dominantly inherited human obesity. Nat. Genet. *20*, 111–112.